

Continuum in the X-Z---Y Weak Bonds: Z= Main Group Elements

Jyothish Joy,^[a] Anex Jose,^[b] and Eluvathingal D. Jemmis^{*[c]}

The Continuum in the variation of the X-Z bond length change from blue-shifting to red-shifting through zero- shifting in the X-Z---Y complex is inevitable. This has been analyzed by *ab-initio* molecular orbital calculations using Z= Hydrogen, Halogens, Chalcogens, and Pnicogens as prototypical examples. Our analysis revealed that, the competition between negative hyperconjugation within the donor (X-Z) molecule and Charge Transfer (CT) from the acceptor (Y) molecule is the primary reason for the X-Z bond length change. Here, we report that, the proper tuning of X- and Y-group for a particular Z- can change the blue-shifting nature of X-Z bond to zero-shifting and further to red-shifting. This observa-

tion led to the proposal of a continuum in the variation of the X-Z bond length during the formation of X-Z---Y complex. The varying number of orbitals and electrons available around the Z-atom differentiates various classes of weak interactions and leads to interactions dramatically different from the H-Bond. Our explanations based on the model of anti-bonding orbitals can be transferred from one class of weak interactions to another. We further take the idea of continuum to the nature of chemical bonding in general. © 2015 Wiley Periodicals, Inc.

DOI: 10.1002/jcc.24036

Introduction

The important role of weak interactions in biology,^[1] material science,^[2] and crystal engineering^[3] has fueled chemists to unravel the mystery behind the origin and nature of such interactions and to explore further. Advancements in experimental and computational techniques helped researchers to search for the new domains of weak interactions. Organic, inorganic, and organometallic complexes with various kinds of weak interactions like H-bonding,^[4,5] halogen-bonding,^[6,7] chalcogen-bonding,^[8–10] pnicogen-bonding,^[11–13] tetrel-bonding,^[14–16] beryllium-bonding,^[17,18] lithium-bonding,^[19–21] boron-bonding,^[22,23] aerogen-bonding^[24] etc. are known today. Theoretical investigations based on the interaction energy and its decomposition into various contributing terms unveiled the nature of interactions at the Z---Y region of X-Z---Y complexes.^[25–28] The nature of X-Z bond length contraction/expansion during the formation of X-Z---Y complex is more involved than in the H-Bond discussed by us earlier.^[4] X-Z---Y complexes have been classified as red-shifting and blue-shifting based on the change in X-Z bond length/vibrational frequency during the complex formation.^[5,9,29,30] Red-shifting complexes show an increase in X-Z bond length and decrease in vibrational frequency on complex formation while blue-shifting complexes show a decrease in X-Z bond length and increase in vibrational frequency. In the context of H-Bonds, the term “proper” X-Z bond is used for complexes that always formed red-shifting Z-Bonds, “pro-improper” X-Z bond for complexes that can be red-shifting or blue-shifting at the equilibrium geometry.^[31,32] Since red- and blue-shifting are either side of the X-Z bond length change, the observation of zero-shift^[4,33–35] imply the inevitability of bond length variation as a continuum ranging from blue- through zero- to red-shifting by properly tuning X- and Y-groups for a particular Z.

Although most of the recent studies on the nature of blue-shifting Z-bonds involve H-bond^[36,37] and halogen-bond^[30,38–40], a few investigations on the blue-shifting nature of chalcogen^[9,25,41,42] bonded complexes are also known. The available explanation for red-shifting is the Charge Transfer (CT) from acceptor group (Y) to the σ^* Anti-Bonding Molecular Orbital (ABMO) of the donor (X-Z) molecule. The extra electron density reaches at the σ^* orbital leads to X-Z bond length elongation. While this explanation for red-shifting is widely accepted, different authors gave different explanations for the existence of blue-shifting.^[31,32,43–46] Some authors proposed that the short range Pauli repulsion (exchange repulsion) is the main reason for blue-shifting H-bond.^[36,43,44,47] Hobza and coworkers argued that a fraction of electron density transferred to the X-H σ^* orbital from the Y-group flows to the other atoms of the X-group, which ultimately leads to blue-shifting.^[31,32] However, this observation was later disproved by Hermansson,^[47] who view blue shifting as a consequence of the interaction between the negative dipole derivative of X-H bond and the electric field exerted by the Y-group along with the short range exchange repulsion. Hermansson's idea of the long range effects of the electric field created by the Y-group

[a] J. Joy

School of Chemistry, Indian Institute of Science Education and Research Thiruvananthapuram, CET Campus, Thiruvananthapuram 695016, Kerala, India

[b] A. Jose

Department of Chemical Sciences, Indian Institute of Science Education and Research-Kolkata, West Bengal 741246, India

[c] E. D. Jemmis

Department of Inorganic and Physical Chemistry, Indian Institute of Science, Bangalore 560012, Karnataka, India
E-mail: jemmis@ipc.iisc.ernet.in

© 2015 Wiley Periodicals, Inc.

is seemingly promising from the Y-group direction but it hardly discusses the electronic structural changes at the X-Z part of the complex. Alabugin et al.^[45,46] and many others^[29,48] viewed blue shifting as a consequence of the rehybridization in the X-H bond based on the Bent's rule. Though there are cases where the rehybridization mechanism based on the Bent's rule does not work for all systems,^[4] many researchers use this concept as a rule of thumb for explaining blue-shifting. The concept of σ -hole^[49,50] helps to understand the nature of noncovalent interactions in many examples. The electron deficient outer area of the Z-atom in the X-Z molecule is described as the σ -hole by Politzer et al.^[51,52] Murray and coworkers^[53] use the concept of σ -hole and the idea of the electric field of the Y-group, proposed by Hermansson^[47] and by Qian and Krimm^[54] to understand the blue shift in the vibrational frequency of a few halogen bonded complexes. The result of unavoidable vibrational mode mixing can be found in their analysis where $\text{O}_2\text{NCl}\cdots\text{NH}_3$ complex is red shifting based on vibrational frequency change, whereas it is blue shifting based on bond length change. The vibrational mode mixing forced researchers to switch the use of vibrational frequency change as a measure of red- or blue-shifting to the X-Z bond length change.^[30,55,56] The lack of an obvious relationship between X-Z bond length change and dipole moment makes it difficult to correlate the nature of blue shifting in bond length to the dipole moment derivative. This realization forced us to analyze the variations in orbital interactions and electron density changes occurring at the X-Z bond during the course of the X-Z \cdots Y complex formation. We have recently analyzed the influence of intramolecular orbital interactions and the electron density reorganization in the X-Z molecule (Z=halogens) and its variations during the complex formation.^[57] We found that, the starting X-Z bond length in the X-Z molecule largely determines the extend and nature of change in the X-Z bond length on X-Z \cdots Y formation and that the Y-group usually influences the magnitude of the effects caused by the X-group for a fixed Z-atom. The starting X-Z bond-lengths, in turn, is controlled by the magnitude of negative hyperconjugation^[58,59] from X-group to X-Z σ^* orbital. Red-shifting is expected in systems where the starting X-Z bond is not excessively long (ie no substantial negative hyperconjugation from X-group to X-Z). However, when the starting X-Z bond is long due to large negative hyperconjugation, the reorganization of electron density in the X-Z group by Y involves depopulation of the X-Z σ^* and results in the shortening of the X-Z bond length. Here, we extend this model to weak interactions involving other Z atoms and show that similar explanations hold for all X-Z \cdots Y complexes considered here with variations in magnitude.

While we largely concentrate on the continuum behavior in the context of examples of X-Z stretch, going from blue-through zero- to red- in the X-Z \cdots Y complexes, we take the idea of continuum further with specific examples. We suggest here that the time has come to treat the range of bonding, from weak to strong bonds, as a part of a larger continuum of the chemical bond.

Methods

Theoretical analyses on all the systems under our investigation are done at *ab-initio* second order Møller-Plesset theory (MP2). All the geometry optimizations and frequency calculations are carried out at MP2(full)/6-311+g(d,p) level of theory without any constraints using Gaussian09 quantum chemistry package.^[60] The selection of this method and basis set is based on two factors. First, it showed good results for comparable molecules. Second, most of the complexes under our discussion are studied in detail by many groups and hence we have recomputed them at a uniform level to substantiate our hypothesis. Basis set superposition Errors (BSSE) are corrected using the standard Counter Poise (CP) correction method of Boys and Bernardi.^[61] Electron Density analysis is performed using AIM2000 program^[62]. Wavefunction files required for AIM analysis are generated from MP2 calculations. NBO6 program^[63] at M06-2x/6-311+g(d,p) level of theory is used to obtain partial atomic population, partial atomic charges, and charge transfer. NBO calculations are done at MP2 optimized geometries using Gaussian09 as the ESS host package. Magnitudes of charge transfer and negative hyperconjugation are obtained from the second order perturbation theory analysis implemented in NBO program.^[64] We have used bond length change as a measure of X-Z bond strength instead of vibrational frequency, due to the unavoidable X-Z stretching mode mixing in the X-Z \cdots Y complex. It was already pointed out by many researchers that, pure X-Z vibrational frequency change during complex formation is only possible for Z=H and mode mixing is unavoidable in other Z-bonds.^[30,55,56]

Energy Decomposition Analysis and Bonding Models

The balance between various forces acting between the X-Z and Y such as electrostatic attraction, orbital interaction, Pauli/exchange repulsion, and dispersion interaction decides the equilibrium X-Z \cdots Y geometry.^[26,28] Even though all the complexes are formed by the balance between the same kind of forces with varying magnitudes, eventually some complexes become red-shifting and some others blue-shifting. Red-shifting can be explained by the higher magnitudes of Charge Transfer (CT) from incoming Y-group to the X-Z σ^* ABMO. Even in the presence of strong CT, some complexes show large blue-shifting (e.g. $\text{O}_2\text{NCl}\cdots\text{NH}_3$). Available models are insufficient to explain similar observations and transfer the idea from one example to another. This situation has motivated us to propose a general analysis that is applicable to all Z-bonds. The CT mechanism of red-shifting complexes prompted us to ask: what if the X-Z σ^* ABMO is partially occupied at the blue-shifting monomer itself. What will happen to this extra electron density at the anti-bonding molecular orbital of X-Z molecule if an electron rich Y-group approaches?

Our analysis on a selected set of blue-shifting Halogen-bonded complexes^[57] evidently showed the presence of negative hyperconjugation from the substituents of X-group

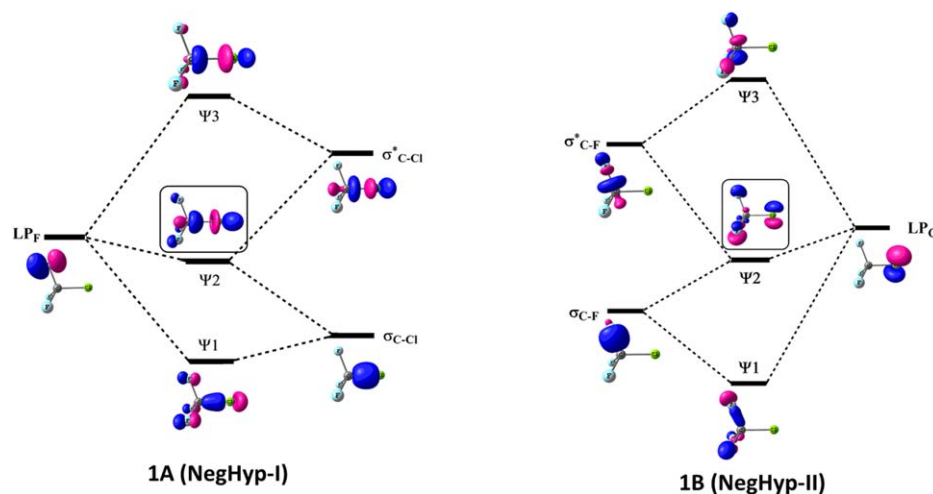


Figure 1. Interaction diagram showing negative hyperconjugative stabilization of F-lone pairs on CF_3 -fragment to the σ^* C-Cl bond (1A) and Cl-lone pair on C-Cl bond to the σ^* C-F bond of CF_3 -fragment (1B) in CF_3Cl molecule.

to the X-Z σ^* orbital in the isolated X-Z molecule itself. This process leads to the partial occupation of X-Z σ^* ABMO and elongation of X-Z bond in the monomer. During the complexation, incoming Y-group perturbs the extra electron density at the X-Z σ^* orbital through long range repulsion by its lone pairs (see Fig. 5 of Ref. [57]). It lead to the shift of electron density at the X-Z σ^* orbital back to X-group itself and hence X-Z bond contraction. This reverse flow decreases the charge density at the Z-atom and excess charge at the X-group, which ultimately led to the electrostatic attraction and hence blue shifting. CT from Y-group has the opposite effect, where it donates electrons to the X-Z σ^* orbital and leads to bond length elongation. Hence, blue-shifting occurs in complexes where the back flow of electrons from X-Z σ^* orbital to X- outweighs CT from Y-group to X-Z σ^* . The opposite scenario leads to red-shifting. In examples where there is no negative hyperconjugation in the parent X-Z, nearly always red-shifting results. With these ideas in mind, and following the terminology used earlier, we have redefined proper X-Z bonded systems as those without negative hyperconjugation. Pro-improper X-Z bonded systems are those with negative hyperconjugation from the substituents of X-group or Z-group/atom. Orbitals participating in negative hyperconjugation from substituents of X-group (1A) as well as that from Z-atom (1B) are shown in Figure 1 using CF_3Cl as a prototype.

Figure 1A shows the negative hyperconjugative stabilization of F- lone pair to the C-Cl σ^* ABMO. It leads to the partial occupation of electron density at the antibonding molecular orbital of C-Cl bond. Figure 1B shows the simultaneous negative hyperconjugative stabilization of lone pair on Cl-atom of C-Cl bond to the C-F σ^* ABMO. This leads to stabilization of C-Cl bond by interacting with the CF_3^- group. Obviously, the observed structure of CF_3Cl is a result of these opposing effects. The incoming Y-group opposite to the direction of C-Cl σ - bond (along the direction of C-Cl σ -hole) leads to two effects, (1) long range repulsion from Y-group activates the back flow of extra electron density at the C-Cl

σ^* orbital (NegHyp-I) and hence bond length contraction, (2) strengthening the process of negative hyperconjugative stabilization of Cl-lone pair to the C-F σ^* ABMO (NegHyp-II). Since process 1A weakens and process 1B strengthens during the formation of X-Z---Y complexation, C-Cl bond compression and blue-shifting occurs. Red-shifting can also be observed in the same system if incoming Y-group can reach very near to C-Cl bond and undergo CT processes. Bond orbitals participating in the above discussed processes (1A and 1B) are shown in Figure. 2.

Above explanations were designed for halogen bonded complexes. Due to the difference in electronegativity and variations in number of electrons and orbitals available for negative hyperconjugation, other Z- bonds (Z= hydrogen, chalcogens, pnictogens, etc.) may show variations compared to halogen bonded complexes. The presence of one electron and one orbital makes hydrogen a unique case in Z-bonds. Unsymmetrically distributed electron pairs in chalcogens and pnictogens may not be able to stabilize its lone pairs as efficiently as halogen. In general, different Z-bonds are expected to show variations in the magnitudes of X-Z bond length change and interaction energy. Herein, we are trying to correlate the factors that influence the X-Z bond length change and

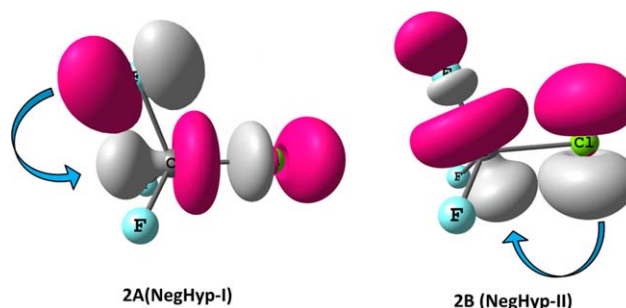


Figure 2. Bond orbitals participating in Negative hyperconjugative donation of electron density from F-lone pair to C-Cl σ^* orbital (2A) and from Cl-lone pair to C-F σ^* orbital (2B) in CF_3Cl molecule. [Color figure can be viewed in the online issue, which is available at [wileyonlinelibrary.com](http://www.wileyonlinelibrary.com).]

Table 1. Geometrical parameters and properties of the model Hydrogen bonded complexes.

No:	Complex	d(H...Y) (Å)	Δ(X-H) (Å)	(X-H...Y) (degree)	B.E _{ZPE-BSSE} (kcal/mol)	Δq _H	Δq _X	Δσ* occupancy	Δ ρ _{BCP} at X-H	CT (kcal/mol)	Δ NegHyp-I (kcal/mol)
1	CCl ₃ H...C ₆ H ₆ ^[65]	2.104	−0.00326	179.99	3.36	0.035	−0.008	−0.00676	0.0032	2.34	−5.13
2	CF ₃ H...C ₆ H ₆ ^[36,45]	2.269	−0.00367	179.55	2.50	+0.027	−0.014	−0.00290	0.0035	1.15	−2.76
3	CF ₃ H...H ₂ O ^[36,45]	2.193	−0.00217	176.39	2.37	0.039	−0.021	−0.00151	0.0036	4.26	−3.01
4	SiF ₃ H...H ₂ O ^[36]	2.507	−0.00154	178.97	0.82	0.031	−0.023	−0.00079	0.0026	2.31	−1.46
5	CCl ₃ H...OMe ₂ ^[66]	2.052	−0.00011	147.01	3.09	0.008	−0.001	−0.00109	0.0023	4.25	−3.89
6	CF ₃ H...NH ₃ ^[45,67]	2.291	−0.00011	179.87	3.04	0.048	−0.03	+0.00278	0.0026	6.59	−3.78
7	SiF ₃ H...NH ₃ ^[36]	2.689	−0.00004	180.00	0.98	0.035	−0.029	+0.00202	0.0027	3.12	−1.65
8	CH ₄ ...H ₂ O ^[44]	2.545	−0.00083	179.92	−0.48	0.024	−0.009	+0.00166	0.0025	1.22	−
9	FH...NH ₃ ^[68]	1.700	+0.03162	180.00	8.13	0.011	−0.067	+0.05746	−0.0473	32.74	−
10	FH...H ₂ O ^[68]	1.731	+0.01488	177.89	4.92	0.019	−0.044	+0.02584	−0.0251	16.19	−
11	CH ₄ ...Cl ^{−[69]}	2.725	+0.0024	180.00	1.60	0.073	−0.019	+0.00799	0.0032	2.87	−
12	NCH...C ₆ H ₆	2.279	+0.0022	179.73	3.16	0.006	−0.009	+0.00484	−0.0013	2.04	+0.74

B.E = Binding Energy. ZPE-BSSE = Zero Point Energy-Basis Set Superposition Error. Δq_H and Δq_X = Change in charge on H-atom and X-group during complexation. Δσ* occupancy = change in the X-H σ* occupancy before and after complex formation. ρ_{BCP} = Density at the Bond Critical Point connecting H and X. CT = Charge Transfer from acceptor to donor. NegHyp = Negative Hyperconjugation. Calculations are done at MP2(full)/6-311+g(d,p) level of theory.

interaction energy during the formation of X-Z...Y complex under the framework of a single explanation. Needless to say, these are only models which help us organize data and think further.

Results and Discussion

Computation on selected sets of hydrogen, halogen, chalcogen, and pnictogen bonded complexes are used as prototypical systems to substantiate our proposed hypothesis. Most of the complexes under our discussions in hydrogen, halogen, and chalcogen are taken from literature. We have designed most of the blue-shifting pnictogen bonded complexes such that it can show maximum negative hyperconjugation and hence blue-shifting. Changes in electronic properties like partial atomic charge (Δq), σ* occupancy (Δσ*) and electron density at the bond critical point (Δρ_{BCP}) on atoms involved in X-Z bond are analyzed. The magnitude of CT from acceptor to donor and changes in negative hyperconjugation (NegHyp-I and NegHyp-II) are the central parameters of the following discussion.

Hydrogen bonds

Compared to other weak Z-bonds, the presence of one electron and one orbital makes H-bonding a special case. Lower electronegativity and unavailability of electrons to participate in NegHyp-II process make for lower magnitudes of X-H bond length compression in blue-shifting cases. Compared to halogens and chalcogens, higher magnitude of binding energy is also expected because of the possibility of large charge polarization available in highly polar X-H bonds. Hydrogen bonded complexes under our discussion are given in Table 1. Incoming Y-groups are selected to represent a wide range of donor abilities ranging from weak to strong.

Changes in the relative magnitude of negative hyperconjugation (Δ NegHyp-I) shows its control over the direction of X-

H bond length (blue-or red-). Blue shift dominates in systems where change in the magnitude of negative hyperconjugation (Δ NegHyp-I) outweigh CT (complex 1 and 2). Comparable values of CT and change in negative hyperconjugation along with reasonable charge separation between X and H lead to lower blue-shifts (complex 3 and 4) or near zero-shifts (complex 5, 6, and 7). The Complex 8 (CH₄...OH₂)^[44] is a special case of blue-shifting H-bonds, where C-H bond contracts even in the absence of negative hyperconjugative donation of electron density to the C-H σ* ABMO. Due to the comparable electronegativity of carbon and hydrogen, CH₄ can be considered as a molecule with uniformly distributed electron density. Any incoming electron rich Y-group can perturb this electron density at the H-atom region of C-H bond and push towards the C-atom region. More electron density reaches the bonding area of C-H bond leads to bond strengthening (blue-shifting). Complex 9, 10, and 11 are proper complexes (red-shifting) with X-H bond elongation. This is due the absence of negative hyperconjugation and higher magnitude of CT. The Complex 12 (NCH...C₆H₆) is a particular case, where C-H σ* orbital is partially occupied by the electron density from N-lone pair. During the complexation, σ* occupancy was found to be increasing along with slight increase in the magnitude of negative hyperconjugation. It leads to the observation of red shift in complex 12.

Analysis of bond critical point (BCP) density is also in line with our arguments where positive values of change in density at the X-H BCP shows an increase in X-H σ-bond strength and hence blue-shifting. Negative values show the decrease in electron density at the X-H bonding region, which represents the extra electron density at the σ* X-H orbital and weakening of X-H bond (red-shifting). Values of the Δ ρ_{BCP} in Table 1 gives clear indication that BCP can be used as a tool for differentiating red-, blue-, or zero- shift in X-H bond length. This observation can be further confirmed by examining the changes in X-H σ* occupancy during the complex formation. Our analysis demonstrates a linear correlation between the

changes in σ^* occupancy and X-H bond length (Supporting Information Fig. S1). Charge analysis shows an attractive interaction between X- and H, irrespective of the red or blue-shifting nature of X-H bonds. Table 1 clearly indicates that complexes where Y-group comes very close to H- of X-H show greater tendency toward red-shifting because of higher possibility for CT (and hence larger interaction energy).

Halogen bonds

The presence of lone pair of electrons around halogen atom of X-Hal molecule makes extra effects which are absent in X-H bonds. All pro-improper halogen bonded molecules show reasonable magnitudes of both the processes (NegHyp-I and NegHyp-II) explained in Figures 1 and 2. Halogen bonded complexes show higher magnitude of blue-shifting and lesser magnitude of interaction energy compared to hydrogen bonded complexes. Both observations can be correlated with the higher electronegativity of halogen atom. Higher electronegativity of Z- atom compared to X creates larger MO coefficient over X- in the X-Z σ^* ABMO. As the size of σ^* lobe over X- increases, magnitude of negative hyperconjugation from substituents on X to X-Z σ^* also increases. Consequently X-Z bond will be elongated in the monomer. Based on our arguments, higher the σ^* occupancy in the monomer greater will be the chance for blue-shifting during the complex formation (X-Z...Y). Higher electronegativity of Z- also decreases the positive electrostatic potential (the σ^- hole) over the Z- atom. As the strength of σ^- hole over the Z-atom decreases, the magnitude of interaction between X-Z and Y also diminishes. This consequently decreases the Interaction Energy (IE). Hence, the

electronegativity of Z-atom has a direct influence over the interaction energy and X-Z bond length change. This is why H-bonded complexes show higher interaction energy and lower blue shifting compared to the halogen-bonded complexes. It is directly reflected in the nature of the continuum plot (Fig. 3). The halogen bonded complexes studied here (Table 2) are in line with the explanations made for H-bonded complexes. Complexes 1 and 21 can be used as representative example for substantiating the arguments based on negative hyperconjugation and CT. Other examples show the gradual transition in the magnitudes of various properties such that the blue-shifting nature changes to zero-shifting and further to red-shifting.

Chalcogen bonds

Since chalcogens are less electronegative than halogens, sigma-hole strength over chalcogen atom in X-Chal will be higher compared to that in halogens and hence larger will be the interaction energy. Lower electronegativity of chalcogens leads to lower σ^* MO coefficients over X-group atom connected to chalcogen, which in turn decreases the magnitude of negative hyperconjugation-I (NegHyp-I). This leads to lower X-Chal σ^* occupancy. The magnitude of NegHyp-II is also found to be low because the lone pair of electrons over chalcogen atom is not properly aligned to have maximum interaction with the ABMOs of X-group. Thus, the magnitude of blue-shifting is found to be lesser in chalcogen bonded complexes compared to halogen bonds.

Red-shifting X-Chal bonds are observed in systems where CT outweigh the total effect of negative hyperconjugations

Table 2. Geometrical parameters and properties of the model Halogen bonded complexes.

Sl no:	Complex	d(Hal...Y) (Å)	$\Delta(X-Hal)$ (Å)	(X-Hal...Y) (degree)	B.E _{ZPE-BSSE} (kcal/mol)	Δq_{Hal}	Δq_X	$\Delta\sigma^*$ occupancy	$\Delta\rho_{BCP}$ at X-Hal	CT (kcal/mol)	Δ NegHyp-I (kcal/mol)	Δ NegHyp-II (kcal/mol)
1	NO ₂ Cl...NH ₃ ^[57]	2.815	-0.0554	179.87	1.27	0.088	-0.041	-0.04708	+0.0224	9.59	-30.62	+5.62
2	NO ₂ Cl...NCH ₃ ^[53]	3.066	-0.0473	179.95	0.84	0.072	-0.027	-0.04812	+0.0157	2.09	-30.23	+5.07
3	HC(O)Cl...NH ₃ ^[70]	3.255	-0.0125	178.39	0.023	0.034	-0.015	-0.00875	+0.0066	1.23	-4.40	+2.83
4	F ₂ NCl...OH ₂ ^[38]	2.829	-0.0107	177.28	1.65	0.033	-0.022	-0.00027	+0.0049	2.39	-2.38	+1.66
5	F ₃ CBr...OH ₂	2.998	-0.0070	179.80	1.57	0.034	-0.018	-0.00455	+0.0040	2.07	-3.48	+1.34
6	CF ₃ Cl...H ₂ O	2.975	-0.0068	179.39	0.88	0.027	-0.013	-0.00416	+0.0041	1.18	-3.64	+1.88
7	CCl ₄ ...NH ₃ ^[67]	2.991	-0.0064	179.99	0.98	0.032	-0.001	+0.00013	+0.0043	3.27	-3.94	+1.58
8	CF ₃ Cl...NH ₃ ^[57]	3.069	-0.0061	179.97	1.23	0.028	-0.015	-0.00024	+0.0042	2.39	-4.12	+1.77
9	PO ₂ Cl...NH ₃	3.083	-0.0059	179.63	1.31	0.029	-0.015	-0.00170	+0.0038	2.62	-3.40	+1.45
10	F ₃ SiCl...OH ₂ ^[30,38]	3.130	-0.0058	179.65	0.26	0.02	-0.013	-0.01310	+0.0023	0.57	-0.90	+1.25
11	F ₃ SiCl...NH ₃ ^[30,67]	3.299	-0.0056	179.99	0.42	0.022	-0.015	+0.00027	+0.0026	1.01	-0.93	+1.38
12	F ₃ CBr...NH ₃	3.031	-0.0044	179.99	2.34	0.034	-0.023	+0.00434	+0.0011	4.73	-4.24	+0.97
13	F ₃ SiBr...NH ₃ ^[67]	3.286	-0.0043	179.99	1.19	0.027	-0.022	+0.00090	+0.0026	1.87	-1.23	+0.81
14	CF ₃ Cl...NMe ₃	2.912	-0.0006	179.47	2.31	0.017	-0.013	+0.00806	+0.0023	3.26	-3.75	+0.51
15	CH ₃ Cl...NH ₃ ^[38,70]	3.312	-0.0007	179.58	-0.69	0.019	-0.011	+0.00379	+0.0018	1.02	-0.12	+0.47
16	CH ₃ Br...NH ₃ ^[38]	3.242	+0.0015	179.99	-0.01	0.024	-0.02	+0.00895	+0.0008	2.31	-0.28	-0.27
17	NH ₂ Cl...NH ₃ ^[70]	3.019	+0.0062	173.98	0.25	0.02	-0.023	+0.01333	-0.0019	2.95	0.00	+2.62
18	FCI...H ₂ O ^[71]	2.581	+0.0152	179.69	3.12	0.007	-0.039	+0.03071	-0.0070	7.86	-	-
19	HOCl...NH ₃ ^[70]	2.712	+0.0210	177.01	2.13	0.008	-0.042	+0.04247	-0.0092	9.07	0.00	+0.01
20	FCI...H ₂ S ^[71]	2.975	+0.0234	178.44	1.52	-0.033	-0.042	+0.07212	-0.0099	12.26	-	-
21	FCI...NH ₃ ^[57,71]	2.306	+0.0719	179.99	6.74	-0.062	-0.106	+0.15953	-0.0291	41.11	-	-

B.E = Binding Energy. ZPE-BSSE = Zero Point Energy-Basis Set Superposition Error. Δq_{Hal} and Δq_X = Change in charge on Hal-atom and X-group during complexation. $\Delta\sigma^*$ occupancy = change in the X-Hal σ^* occupancy before and after complex formation. ρ_{BCP} = Density at the Bond Critical Point connecting Hal- and X. CT = Charge Transfer from acceptor to donor. NegHyp = Negative Hyperconjugation. Calculations are done at MP2(full)/6-311+g(d,p) level of theory.

Table 3. Geometrical parameters and properties of the model Chalcogen bonded complexes.

Sl. No	Complex	d(Chl...Y) (Å)	$\Delta(X\text{-}Chl)$ (Å)	(X-Chl...Y) (degree)	B.E _{ZPE-BSSE} (kcal/mol)	Δq_{Chl}	Δq_X	$\Delta\sigma^*$ occupancy	$\Delta\rho_{BCP}$ at X-Chl	CT (kcal/mol)	$\Delta NegHyp-I$ (kcal/mol)	$\Delta NegHyp-II$ (kcal/mol)
1	NO ₂ SMe...OH ₂	3.068	−0.0040	178.04	2.06	0.021	−0.009	−0.00785	+0.0002	2.13	−3.99	+1.75
2	NO ₂ SMe...FH	3.188	−0.0038	177.70	1.56	0.010	−0.005	−0.00521	+0.0006	0.82	−2.20	+1.38
3	NO ₂ SMe...NH ₃ ^[41]	3.108	−0.0034	176.05	2.50	0.021	−0.010	−0.00563	+0.0002	2.84	−4.35	+1.87
4	CF ₃ SMe...NH ₃ ^[41]	3.339	−0.0022	175.88	1.99	0.000	−0.004	−0.00021	+0.0004	0.72	−0.96	+0.65
5	CF ₃ MeS...OH ₂	3.215	−0.0021	173.38	1.59	0.009	−0.007	−0.00093	+0.0004	1.01	−1.19	+0.63
6	CF ₃ MeS...FH	3.284	−0.0015	159.45	0.62	0.008	−0.001	−0.00043	+0.0005	0.37	−0.14	−1.6
7	NO ₂ SMe...OMe ₂	2.857	−0.0013	177.68	3.23	0.014	−0.009	−0.00284	−0.0006	2.79	−4.26	+0.69
8	CF ₃ MeS...OMe ₂	3.016	−0.0007	176.65	2.63	0.002	−0.005	0.00148	+0.0001	1.18	−1.14	+0.31
9	CF ₃ MeS...NMe ₃	3.033	0.0018	173.79	2.99	0.014	−0.008	0.00444	−0.0007	2.17	−1.60	+0.9
10	NH ₂ SMe...NH ₃ ^[41]	3.419	0.0023	171.08	0.81	−0.011	0.000	0.00213	−0.0009	0.25	0.0	−0.41
11	H ₂ CS...Cl ^[9]	3.569	0.0039	179.98	−0.78	0.120	−0.091	0.00709	−0.0030	1.65	0.0	+4.28
12	OHSM...NH ₃ ^[41]	3.245	0.0061	174.89	1.44	0.000	−0.009	0.00491	−0.0022	1.12	0.0	−0.26
13	MeSH...NH ₃ ^[41,42]	3.384	0.0086	158.62	1.99	−0.018	0.001	0.00153	−0.0008	0.35	0.0	−0.87
14	CISMe...NH ₃ ^[41]	3.041	0.0128	173.52	1.90	0.010	−0.028	0.01357	−0.0035	3.09	0.00	−0.28
15	NO ₂ SMe...NMe ₃	2.718	0.0155	173.79	3.97	0.020	−0.012	0.01551	−0.0065	9.51	−6.20	−0.40
16	FSMe...NH ₃ ^[41]	2.827	0.0212	176.57	2.43	0.006	−0.031	0.02290	−0.0066	6.67	0.0	−0.71
17	CISH...NH ₃ ^[42]	2.719	0.0319	167.9	2.91	0.014	−0.067	0.05059	−0.0087	10.93	0.0	0.0
18	FSH...NH ₃ ^[42]	2.529	0.03801	169.48	4.96	−0.022	−0.059	0.07469	−0.0117	18.67	0.0	0.0

B.E = Binding Energy. ZPE-BSSE = Zero Point Energy-Basis Set Superposition Error. Δq_{Chl} and Δq_X = Change in charge on Chl-atom and X-group during complexation. $\Delta\sigma^*$ occupancy = change in the X-Chl σ^* occupancy before and after complex formation. ρ_{BCP} = Density at the Bond Critical Point connecting Chl- and X. CT = Charge Transfer from acceptor to donor. NegHyp = Negative Hyperconjugation. Calculations are done at MP2(full)/6-311+g(d,p) level of theory.

(NegHyp-I and NegHyp-II). This can be evidently observed by comparing complexes 3 and 15. In the case of NO₂SMe...NH₃ complex, NegHyp-I has larger magnitude than CT, but replacing NH₃ with NMe₃ reverses the situation where highly electron donating NMe₃ override the Negative Hyperconjugation and hence red-shifting in N-S bond length. Analysis of natural charge and changes in the density at Bond Critical Point (BCP) also support our arguments.

Pnicogen bonds

Blue-shifting X-Pni bonds are rare. Lower electronegativity of pnicogen atoms compared to other Z-atoms (Z=H, halogen, chalcogen) is the main reason for this observation. X-Pni...Y complexes with usual X-groups that can show blue-shifting in other Z-bonds are not blue-shifting here. Lower electronegativity of pnicogens leads to larger MO coefficients over pnicogen atom in X-Pni σ^* ABMO. This in turn leads to an increase in the extent of CT acceptance from Y-group and hence more chance for red-shifting. On the other hand, lower MO coefficient over X-atom decreases the extent of negative hyperconjugation from its substituents to the X-Pni σ^* orbital. Hence, it is difficult to observe blue-shifted Pnicogen bonded complexes.

It can be noticed from Table 4 that Phosphorus prefers Silicon-based molecular fragments as X-group for blue-shifting. This is due to the lower electronegativity of Silicon compared to Phosphorus where negative hyperconjugation (NegHyp-I) is available (Table 4, examples 1-4). This conclusively proves that the negative hyperconjugation is a pre-requisite for blue shift in X-Z molecule. Our analysis also gives explanation to the question of why complexes 8, 15, and 16 show decrease in

binding energy as number of fluorine substituents increases.^[72] It is very common to expect that as the number of fluorine atoms connected to phosphorus increases, σ -hole strength increases and hence higher interaction energy, but reverse is observed in this case. The reason for the above observation can be obtained by analyzing the CT values. Stabilization due to CT is decreasing as the number of fluorine atoms increases. The σ^* -orbital on the donor molecule (X-Pni) which has to receive the electron density become more and more destabilizes as the number of Fluorine atoms increases. This creates an orbital mismatch between the lone pair orbital on the acceptor molecule (Y) and X-P σ^* -ABMO. Thus, the increase in orbital energy mismatch leads to decrease in the magnitude of CT stabilization and hence lower binding energy. Complexes 1 and 18 give representative examples where blue-shifting systems can be converted to red-shifting by proper substitution.

The nature of the Z-bond in X-Z...Y for other elements can be analyzed in a similar fashion. One of the well-studied classes of Z-bonds apart from the ones discussed is Li-bonds.^[19,73] Electrostatics is the major attractive interaction whereas CT is of less importance here. Vibrational mode mixing is one of the reasons for the observation of blue-shifting in the X-Li vibrational frequency with increased bond length (red-shifting in bond length).^[73-75] Feng et al.^[21] analyzed a few Li-bonded complexes in detail and observed systems with shortened X-Li bond. The examples given by Feng and coworkers for blue-shifting Li-bonded complexes can be understood by following our analysis. So far there is no literature report about blue-shifting beryllium or boron bonds. Our analysis showed the indications of blue shifting/zero-shifting in C-Be bond of F₃CBeH...Ne complex (−0.0004 Å). Though we

Table 4. Geometrical parameters and properties of the model Pnictogen bonded complexes.

Si.No	Complex	d(Pni...Y) (Å)	$\Delta(X-Pni)$ (Å)	(X-Pni...Y) (degree)	B.E _{ZPE-BSSE} (kcal/mol)	Δq_{Pni}	Δq_X	$\Delta \sigma^*$ occupancy	$\Delta \rho_{BCP}$ at X-Pni	CT (kcal/mol)	$\Delta NegHyp-I$ (kcal/mol)	$\Delta NegHyp-II$ (kcal/mol)
1	PH ₂ SiCl ₃ -FLi	2.836	-0.0033	152.76	3.88	0.051	-0.017	-0.00443	0.0034	2.46	-4.30	+1.30
2	PH ₂ SiBr ₃ -FH	3.245	-0.0025	139.16	0.48	0.005	0.001	-0.00290	0.0009	0.24	-0.23	+0.39
3	PH ₂ SiCl ₃ -FNa	2.658	-0.0016	157.29	5.68	0.082	-0.028	-0.00096	0.0039	5.34	-5.43	+1.77
4	PH ₂ SiBr ₃ -FLi	2.793	-0.0013	154.33	4.07	0.059	-0.008	-0.00453	0.0030	3.02	-2.85	+1.65
5	PH ₂ CF ₃ -FH	3.161	-0.0005	147.74	0.90	0.003	-0.005	-0.00021	-0.0006	0.78	-0.62	+0.17
6	PH ₂ SiCl ₃ -NH ₃	3.257	-0.0002	157.17	1.05	0.020	-0.007	0.00152	0.0019	2.48	-2.84	+0.54
7	PH ₂ Cl-NH ₃ ^[12,76-78]	2.749	0.0379	164.81	2.77	0.022	-0.062	0.04538	-0.0087	11.08	0.00	0.00
8	PH ₂ F-NH ₃ ^[12,76-80]	2.662	0.0267	165.94	3.61	-0.014	-0.037	0.04711	-0.0078	11.95	0.00	0.00
9	PH ₂ SiF ₃ -FLi	2.905	0.0005	148.82	4.27	0.036	-0.041	0.00056	0.0028	1.55	-1.82	+0.56
10	PH ₂ CCl ₃ -H ₂ O	2.926	0.0032	160.91	1.60	0.016	-0.002	0.00470	-0.0018	3.49	-1.12	+0.55
11	PH ₂ CCl ₃ -NH ₃	2.938	0.0093	162.60	2.14	0.022	-0.004	0.01735	-0.0033	6.30	-1.54	+0.66
12	PH ₂ SiCl ₃ -NMe ₃	2.902	0.0093	159.59	2.03	0.030	-0.007	0.01033	0.0017	4.49	-3.57	+0.45
13	PH ₂ CN-NH ₃ ^[77]	3.001	0.0148	161.62	2.69	0.012	0.0	0.01815	-0.0043	5.13	-0.46	+0.02
14	PH ₂ OH-NH ₃ ^[12,78]	2.886	0.0163	163.41	1.69	0.005	-0.027	0.02560	-0.0051	6.38	0.0	0.00
15	PF ₃ -NH ₃ ^[76,77]	2.841	0.0171	168.55	2.52	0.019	-0.020	0.00527	-0.0054	3.46	-1.69	0.00
16	PHF ₂ -NH ₃ ^[76,77]	2.753	0.0201	165.15	3.35	0.006	-0.026	0.01931	-0.0063	6.61	-0.79	0.00
17	PCN ₃ -NH ₃ ^[77]	2.778	0.0215	165.53	6.84	0.020	-0.003	0.02579	-0.0057	7.81	-1.26	-1.51
18	PH ₂ NO ₂ -NH ₃ ^[12,78]	2.659	0.0217	163.91	4.44	0.017	-0.015	0.03502	-0.0069	15.04	-1.61	+0.16

B.E = Binding Energy. ZPE-BSSE = Zero Point Energy-Basis Set Superposition Error. Δq_{Pni} and Δq_X = Change in charge on Pni-atom and X-group during complexation. $\Delta \sigma^*$ occupancy = change in the X-Pni σ^* occupancy before and after complex formation. ρ_{BCP} = Density at the Bond Critical Point connecting Pni- and X. CT = Charge Transfer from acceptor to donor. NegHyp = Negative Hyperconjugation. Calculations are done at MP2(full)/6-311+g(d,p) level of theory.

have not discussed in the article, carbon-bonds also follow the same trend (Supporting Information Table S1). Thus, we suggest that the idea of electron density reorganization at the X-Z bonding region during the course of X-Z...Y complex formation can be attributed to the root cause of bond length change. The magnitude and direction of the change in bond length can be understood by following our analysis.

As a summary, we observed a linear correlation between the changes in X-Z bond length and σ^* ABMO electron density (Supporting Information Fig. S1). Hence, the various factors that influences the X-Z σ^* occupancy decides the nature of X-Z bond length change in the X-Z...Y complex. Negative hyperconjugation from the X-group leads to the extra electron density at ABMO of X-Z bond. Incoming Y-group pushes this extra electron density back to the X-group by long range repulsion,^[57] as well as by short range Pauli/exchange interaction.^[47] Removal of the extra electron density at the σ^* ABMO leads to blue shifting along with the electrostatic attraction between X- and Z. The short range charge transfer from Y-group to X-Z ABMO leads to concomitant increase in the X-Z σ^* ABMO occupancy, which consequently leads to red-shifting. Hence, the proper balance between the electron density at the X-Z σ^* ABMO in parent X-Z molecule and its complexed form (X-Z...Y) decides the blue-, zero- or red- shifting nature.

Factors Influencing the Continuum Nature of X-Z Bond Length Change

As we have implied before,^[4,33,57] analysis of various classes of weak interactions buttresses the fact that, there exists a continuum of bond length variation from blue- through zero- to red- shifting during X-Z...Y complex formation. The X- and Y-group has subtle effects on the continuum nature of X-Z...Y.

The Y-group influences the magnitude of X-Z bond length change in two ways, at larger separations, the long range repulsion between lone pair electrons on Y-group and the extra electron density at the σ^* ABMO of X-Z bond triggers the flow of electron density from X-Z σ^* to the substituents on X (assuming the monomer X-Z has reasonable amount of negative hyperconjugation). This leads to the X-Z bond length compression. At shorter separations, a second factor viz CT from the lone pair of electrons on Y-group to the σ^* ABMO of X-Z bond becomes stronger and leads to bond length elongation. Hence, the proper balance between the short and long range effects of Y- group can decide the X-Z bond length change direction as well as the equilibrium X-Z...Y geometry.

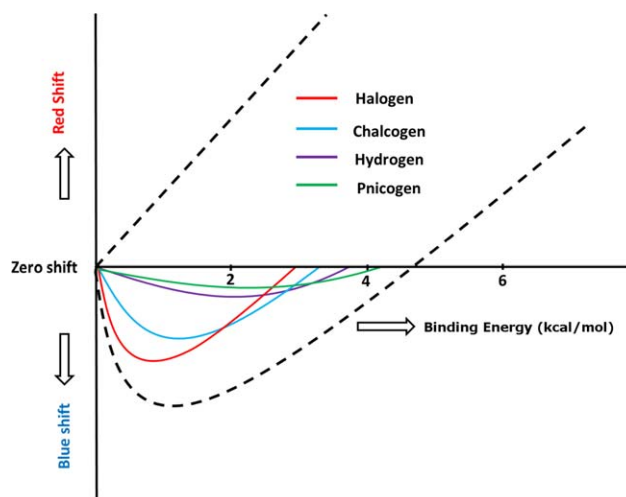


Figure 3. Pictorial representation of the variations in the magnitudes of X-Z bond length with interaction energy during the formation of different sets of weakly interacting complexes.

Energetics of the interaction at the equilibrium $X-Z\cdots Y$ geometry is decided by the various forces acting at the $Z\cdots Y$ region, like electrostatic attraction, Pauli/exchange repulsion, orbital interactions, dispersion interactions etc.^[7,26,27] Most of these effects are controlled by the electronegativity of the Z-atom. Highly electronegative Z-atom avoids large σ -hole over the Z-atom of X-Z molecule. This leads to lesser electrostatic attraction between Z- and Y-group. This also increases the Pauli repulsion between the monomers and leads to the mutual repulsion between the X-Z and Y. Hence, the resultant larger separation between the monomers leads to lower magnitude of interaction energy. Thus, the magnitude of interaction energy and equilibrium monomer separation is decided by the electronegativity of the Z-atom and the ability of Y-group to donate its lone pair electron density.

The nature of X-group is the ultimate factor that controls both the above mentioned effects of Y-group and Z-atom. The reason for the above argument is that, negative hyperconjugation is the unique property of X-group and blue-shifting would not have been possible in most cases without the presence of negative hyperconjugation from X-group. In order to have reasonable interaction energy with optimum blue-shifting, X-groups has to be selected in such a way that, the group electronegativity of X- should be strong enough to make a sigma hole over the Z-atom and the electronegativity of X-group atom directly connected to Z-atom should be less than that of Z-atom. A comparison between different classes of $X-Z\cdots Y$ interactions by keeping X-group as NO_2 and Y-group as NH_3 for different Z-atoms can be found in Supporting Information Table S2.

A qualitative drawing of the continuum nature of weak interactions for different classes of complexes can be seen in Figure 3 (The distribution of the complexes studied in the present analysis can be found in Supporting Information Fig. S2). The black dashed lines represent the broad picture of continuum ranging from blue- through zero- to red- shifting. The positive quadrant represents the region where red-shift in X-Z bond with diverse interaction energies. The lower negative quadrant is intentionally partitioned in to a curved area to emphasize the limited spread of blue-shifting complexes wherein the higher energy analogs are expected to be red-shifting. This qualitative diagram points the inevitability of bond length change from blue- shifting to red-shifting through zero-shifting. Colored lines represent the selective behavior of each class of interactions towards blue- shifting. Halogen-bonded complexes show larger magnitude of blue-shifting with smaller interaction energy compared to chalcogen-bonded complexes, which is followed by hydrogen-bonds and pnictogen-bonds. It is clear from the above explanations that, higher the electronegativity of Z-atom, lesser will be the interaction energy and more will be the magnitude of blue-shifting. Each curve representing weak interactions of a selected category of Z-atom starts from blue-shifting and passes through a region in the X-axis corresponding to zero-shift. Here, the X-Z bond length remains unchanged in the complex with non-zero, though small, interaction energy, a position at which forces that lengthen the X-Z bond equal the

Table 5. Variations in the bonding properties of X_3B and Y during the conversion of strong $X_3B\leftarrow Y$ to weak $X_3B\cdots Y$.

Complex $X_3B\cdots Y$	$d(B\cdots Y)$ (Å)	$B.E_{ZPE-BSE}$ (kcal/mol)	$\Delta(<XB X)$ (degrees)	$\Delta d(B-X)$ (Å)
$H_3B\cdots NH_3$	1.653	21.71	-6.27	+0.0183
$F_3B\cdots NH_3$	1.665	13.96	-5.80	+0.0596
$F_3B\cdots NCH$	2.434	2.97	-3.43	+0.0059
$F_3B\cdots N_2$	2.791	0.97	-0.85	+0.0010

Calculations are done at MP2(full)/6-311+g(d,p) level of theory.

forces that shorten the same. We have calculated several examples with nearly zero-shift in the X-Z stretch, with non-zero interaction energy for all classes of $X-Z\cdots Y$ complexes (Tables 1–4). There are a couple of experimental complexes with near zero-shift.^[34,35]

In principle, the arguments we made here can be extended to any element in the periodic table. It is clear that for any element Z- a proper set of X- and Y- group can be designed to stabilize an $X-Z\cdots Y$ complex, generating Z-bonds. The discovery of tetrel-bonding,^[14,15,81] boron-bonding,^[22,82] aerogen-bonding^[24] etc. are the recently added new members to the family of weak interactions. We anticipate that, with time, Z-bonds of other elements will be identified.

Continuum Nature of Bonding

We want to point out another aspect of continuum in the nature of chemical bonding. The gradation from a regular 2-center 2-electron bond to a Z-Bond (be it weak or strong) is not discontinuous. Though at first a coordinate bond such as the N-B bond in $H_3B\leftarrow NH_3$ appears very distinct from a Z-bond, the difference vanishes for several of its derivatives. The complex formed between NH_3 and BF_3 show a strong coordinate-covalent bond. The nature of bonding involved in $X_3B\leftarrow Y$ alters dramatically when NH_3 is replaced with NCH or N_2 as electron donors. Our analysis about the bonding nature in $X_3B\leftarrow Y$ complexes is given in Table 5. Separation between the monomers increases to the van der Waals region, changes in the geometrical parameters disappears and interaction energy goes down to a weak H-bonding region. This clearly shows that the proper tuning of substituents on B- and the nature of incoming Y-group can change the strong bonding nature of $X_3B\leftarrow Y$ to a weak bonding $X_3B\cdots Y$. Recently, Grabowski showed the existence of weak triel-bonds^[22] (weak bonds involving Group-III atoms). His analysis shed light in to the existence of weak boron-bonds, though the continuum nature of 2-centre 2-electron and Z-bond was not obvious. Very recently Chalmers et al., observed the strong-bond to dative-bond and further to no-bond interactions in constrained P---Sb systems as the Lewis acidity of the acceptor decreases.^[83] Similar observations can be made about the course of atom abstraction reactions,^[84] chemical reaction mechanisms^[85] or nucleophilic substitution reactions^[86] published in recent times. All these observations call for a

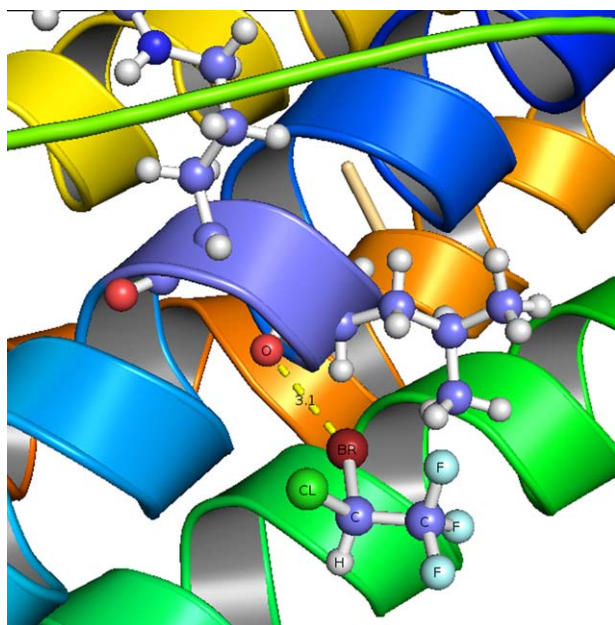


Figure 4. Protein structure (PDB ID: 1XZ1^[87]) showing the presence of a blue shifted Halogen bond (Br...O bond). [Color figure can be viewed in the online issue, which is available at wileyonlinelibrary.com.]

generalization of the continuum nature of the chemical bond, uniting weak and strong chemical interactions.

Conclusions

The reasons for the change in X-Z bond length of X-Z...Y complex has been analyzed using the LCAO-MO model and verified by *ab-initio* molecular orbital calculations. The existence of negative hyperconjugation from X-group to X-Z σ^* ABMO in the isolated X-Z molecule is the primary factor that classifies X-Z as proper and pro-improper Z-bond partner. The balance between the flow of electron density accumulated in the σ^* ABMO of X-Z from negative hyperconjugation back to the X group, and the CT from Y-group to the X-Z σ^* ABMO, decides the blue-shifting or red-shifting nature of the X-Z bond in the X-Z...Y complex. Our analysis of the change of X-Z bond length from blue-shifting to red-shifting through zero-shifting for Z=hydrogen-, halogen-, chalcogen-, and pnictogen- bonded complexes led to the understanding of the crucial role played by the electronegativity of Z-atom in deciding the nature of different weak interactions. This can be used in designing new weakly interacting complexes with varying magnitudes of X-Z bond length and interaction energies. The explanations used here can be transferred from one variety of weak interactions to another. A number of blue-shifted Halogen-bonded Protein-Ligand interactions are found in the Protein Data Bank (PDB), like the one shown in Figure 4. Our study calls for the proper parameterization of the existing force fields to include the effects of blue shifting X-Z bonds. Just as the existence of a continuum of behavior in weak interactions is inevitable, we propose the idea that strong conventional bonds and weak Z-Bonds form literally a part of the continuum that the nature of chemical bond presents.


Acknowledgments

The authors thank IISER-TVM, IISc-Bangalore and CMSD-Hyderabad for computational facilities. EDJ thanks the DST for funding through the J. C. Bose Fellowship. AJ thanks DST for INSPIRE fellowship and IASc for summer research fellowship. JJ thanks UGC-India for Senior Research Fellowship.

Dedication: This article is respectfully dedicated to the memory of Professor Paul von Ragué Schleyer, and to Mrs Inge Schleyer who took me (EDJ) as a stay-in-house Ph.D. student.

Keywords: continuum • weak interactions • red- and blue-shift • negative hyperconjugation • charge transfer

How to cite this article: J. Joy, A. Jose, E. D. Jemmis. *J. Comput. Chem.* **2016**, 37, 270–279. DOI: 10.1002/jcc.24036

 Additional Supporting Information may be found in the online version of this article.

- [1] G. A. Jeffrey, W. Saenger, *Hydrogen Bonding in Biological Structures*; Springer-Verlag: Berlin, New York, **1994**.
- [2] S. Srivastava, *Recent Development in Material Science*; Research India Press: New Delhi, **2011**.
- [3] G. R. Desiraju, J. J. Vittal, A. Ramanan, *Crystal Engineering: A textbook*; World Scientific, IISc Press: New Jersey, N.J., **2011**.
- [4] J. Joseph, E. D. Jemmis, *J. Am. Chem. Soc.* **2007**, 129, 4620.
- [5] P. Hobza, Z. Havlas, *Chem. Rev.* **2000**, 100, 4253.
- [6] P. Metrangola, G. Resnati, *Cryst. Growth Des.* **2012**, 12, 5835.
- [7] P. Politzer, J. S. Murray, T. Clark, *Phys. Chem. Chem. Phys.* **2010**, 12, 7748.
- [8] C. Bleiholder, D. B. Werz, H. Köppel, R. Gleiter, *J. Am. Chem. Soc.* **2006**, 128, 2666.
- [9] W. Wang, B. Ji, Y. Zhang, *J. Phys. Chem. A* **2009**, 113, 8132.
- [10] M. E. Brezgunova, J. Lieffrig, E. Aubert, S. Dohaoui, P. Fertey, S. Lebègue, J. G. Ángyán, M. Fourmigué, E. Espinosa, *Cryst. Growth Des.* **2013**, 13, 3283.
- [11] J. E. Del Bene, I. Alkorta, G. Sanchez-Sanz, J. Elguero, *J. Phys. Chem. A* **2011**, 115, 13724.
- [12] S. Scheiner, *J. Phys. Chem. A* **2011**, 115, 11202.
- [13] S. Scheiner, *J. Chem. Phys.* **2011**, 134, 164313.
- [14] A. Bauzá, T. J. Mooibroek, A. Frontera, *Angew. Chem. Int. Ed.* **2013**, 52, 12317.
- [15] D. Mani, E. Arunan, *Phys. Chem. Chem. Phys.* **2013**, 15, 14377.
- [16] S. P. Thomas, M. S. Pavan, T. N. Guru Row, *Chem. Commun.* **2014**, 50, 49.
- [17] E. F. Villanueva, O. Mo, M. Yanez, *Phys. Chem. Chem. Phys.* **2014**, 16, 17531.
- [18] M. Yáñez, P. Sanz, O. Mó, I. Alkorta, J. Elguero, *J. Chem. Theory Comput.* **2009**, 5, 2763.
- [19] A. B. Sannigrahi, T. Kar, B. G. Niyogi, P. Hobza, P. v. R. Schleyer, *Chem. Rev.* **1990**, 90, 1061.
- [20] J. Wu, H. Yan, H. Chen, A. Zhong, W. Cao, *Comp. Theor. Chem.* **2012**, 1000, 52.
- [21] Y. Feng, L. Liu, J.-T. Wang, X.-S. Li, Q.-X. Guo, *Chem. Commun.* **2004**, 1, 88.
- [22] S. J. Grabowski, *ChemPhysChem* **2014**, 15, 2985.
- [23] S. J. Grabowski, *ChemPhysChem* **2015**, 16, 1470.
- [24] A. Bauzá, A. Frontera, *Angew. Chem. Int. Ed.* **2015**, 54, 7340.
- [25] S. Scheiner, *Int. J. Quantum Chem.* **2013**, 113, 1609.
- [26] S. M. Huber, J. D. Scanlon, E. Jimenez-Izal, J. M. Ugalde, I. Infante, *Phys. Chem. Chem. Phys.* **2013**, 15, 10350.
- [27] M. D. Esrafil, B. Ahmadi, *Comp. Theor. Chem.* **2012**, 997, 77.
- [28] D. R. Duarte, G. Sosa, N. Peruchena, *J. Mol. Model.* **2013**, 19, 2035.

- [29] S. J. Grabowski, *J. Phys. Chem. A* **2011**, *115*, 12789.
- [30] W. Wang, N.-B. Wong, W. Zheng, A. Tian, *J. Phys. Chem. A* **2004**, *108*, 1799.
- [31] B. J. van der Veken, W. A. Herrebout, R. Szostak, D. N. Shchepkin, Z. Havlas, P. Hobza, *J. Am. Chem. Soc.* **2001**, *123*, 12290.
- [32] W. Zierkiewicz, D. Michalska, Z. Havlas, P. Hobza, *ChemPhysChem* **2002**, *3*, 511.
- [33] K. Sundararajan, N. Ramanathan, K. S. Viswanathan, K. Vidya, E. D. Jemmis, *J. Mol. Struct.* **2013**, *1049*, 69.
- [34] M. M. Nolasco, P. J. A. Ribeiro-Claro, *ChemPhysChem* **2005**, *6*, 496.
- [35] M. D. Struble, C. Kelly, M. A. Siegler, T. Lectka, *Angew. Chem., Int. Ed.* **2014**, *53*, 8924.
- [36] X. Li, L. Liu, H. B. Schlegel, *J. Am. Chem. Soc.* **2002**, *124*, 9639.
- [37] Y. Mo, C. Wang, L. Guan, B. Braida, P. C. Hiberty, W. Wu, *Chem. Eur. J.* **2014**, *20*, 8444.
- [38] W. Wang, P. Hobza, *J. Phys. Chem. A* **2008**, *112*, 4114.
- [39] C. Wang, D. Danovich, Y. Mo, S. Shaik, *J. Chem. Theory Comput.* **2014**, *10*, 3726.
- [40] D. Hauchecorne, W. A. Herrebout, *J. Phys. Chem. A* **2013**, *117*, 11548.
- [41] U. Adhikari, S. Scheiner, *J. Phys. Chem. A* **2014**, vol. 118, 3183.
- [42] U. Adhikari, S. Scheiner, *J. Phys. Chem. A* **2012**, *116*, 3487.
- [43] S. Scheiner, S. J. Grabowski, T. Kar, *J. Phys. Chem. A* **2001**, *105*, 10607.
- [44] Y. Gu, T. Kar, S. Scheiner, *J. Am. Chem. Soc.* **1999**, *121*, 9411.
- [45] I. V. Alabugin, M. Manoharan, S. Peabody, F. Weinhold, *J. Am. Chem. Soc.* **2003**, *125*, 5973.
- [46] I. V. Alabugin, S. Bresch, M. Manoharan, *J. Phys. Chem. A* **2014**, *118*, 3663.
- [47] K. Hermansson, *J. Phys. Chem. A* **2002**, *106*, 4695.
- [48] S. J. Grabowski, *J. Phys. Chem. A* **2011**, *115*, 12340.
- [49] T. Clark, M. Hennemann, J. Murray, P. Politzer, *J. Mol. Model.* **2007**, *13*, 291.
- [50] P. Politzer, J. S. Murray, P. Lane, *Int. J. Quantum Chem.* **2007**, *107*, 3046.
- [51] P. Politzer, P. Lane, M. Concha, Y. Ma, J. Murray, *J. Mol. Model.* **2007**, *13*, 305.
- [52] J. Murray, P. Lane, P. Politzer, *J. Mol. Model.* **2009**, *15*, 723.
- [53] J. Murray, M. Concha, P. Lane, P. Hobza, P. Politzer, *J. Mol. Model.* **2008**, *14*, 699.
- [54] W. Qian, S. Krimm, *J. Phys. Chem. A* **2002**, *106*, 6628.
- [55] B. Ji, Y. Zhang, D. Deng, W. Wang, *Cryst. Eng. Comm.* **2013**, *15*, 3093.
- [56] B. Raghavendra, E. Arunan, *J. Phys. Chem. A* **2007**, *111*, 9699.
- [57] J. Joy, E. D. Jemmis, K. Vidya, *Faraday Discuss.* **2015**, *177*, 33.
- [58] I. Fleming, *Molecular Orbitals and Organic Chemical Reactions*; Wiley: Chichester, West Sussex, U.K., **2009**.
- [59] A. D. McNaught, A. Wilkinson, *Compendium of Chemical Terminology: IUPAC Recommendations*; Blackwell Science, Oxford England; Malden, MA, USA, **1997**.
- [60] M. J. Frisch, G. W. Trucks, H. B. Schlegel, G. E. Scuseria, M. A. Robb, J. R. Cheeseman, G. Scalmani, V. Barone, B. Mennucci, G. A. Petersson, H. Nakatsuji, M. Caricato, X. Li, H. P. Hratchian, A. F. Izmaylov, J. Bloino, G. Zheng, J. L. Sonnenberg, M. Hada, M. Ehara, K. Toyota, R. Fukuda, J. Hasegawa, M. Ishida, T. Nakajima, Y. Honda, O. Kitao, H. Nakai, T. Vreven, J. A. Montgomery, J. E. Peralta, F. Ogliaro, M. Bearpark, J. J. Heyd, E. N. Brothers, K. N. Kudin, V. N. Staroverov, R. Kobayashi, J. Normand, K. Raghavachari, A. P. Rendell, J. C. Burant, S. S. Iyengar, J. Tomasi, M. Cossi, N. Rega, J. M. Millam, M. Klene, J. E. Knox, J. B. Cross, V. Bakken, C. Adamo, J. Jaramillo, R. Gomperts, R. E. Stratmann, O. Yazyev, A. J. Austin, R. Cammi, C. Pomelli, J. W. Ochterski, R. L. Martin, K. Morokuma, V. G. Zakrzewski, G. A. Voth, P. Salvador, J. J. Dannenberg, S. Dapprich, A. D. Daniels, Ö. Farkas, J. B. Foresman, J. V. Ortiz, J. Cioslowski, D. J. Fox, Gaussian 09 Revision D.01; Gaussian, Inc.: Wallingford, CT, **2013**.
- [61] S. F. Boys, F. Bernardi, *Mol. Phys.* **1970**, *19*, 553.
- [62] F. Biegler-König, J. Schönbohm, *J. Comput. Chem.* **2001**, *22*, 545.
- [63] E. D. Glendening, C. R. Landis, F. Weinhold, *J. Comput. Chem.* **2013**, *34*, 1429.
- [64] E. D. Glendening, J. K. Badenhoop, A. E. Reed, J. E. Carpenter, J. A. Bohmann, C. M. Morales, C. R. Landis, F. Weinhold, NBO 6.0. Theoretical Chemistry Institute; University of Wisconsin: Madison, **2013**.
- [65] A. J. Barnes, *J. Mol. Struct.* **2004**, *704*, 3.
- [66] S. N. Delanoye, W. A. Herrebout, B. J. van der Veken, *J. Am. Chem. Soc.* **2002**, *124*, 7490.
- [67] W. Wang, Y. Zhang, B. Ji, *J. Phys. Chem. A* **2010**, *114*, 7257.
- [68] G. R. Desiraju, T. Steiner, *The Weak Hydrogen Bond: In Structural Chemistry and Biology*; Oxford University Press: Oxford; New York, **1999**.
- [69] P. Hobza, Z. Havlas, *Theor. Chem. Acc.* **2002**, *108*, 325.
- [70] J.-W. Zou, Y.-J. Jiang, M. Guo, G.-X. Hu, B. Zhang, H.-C. Liu, Q.-S. Yu, *Chem. Eur. J.* **2005**, *11*, 740.
- [71] N. J. M. Amezcaga, S. C. Pamies, N. I. M. Peruchena, G. L. Sosa, *J. Phys. Chem. A* **2009**, *114*, 552.
- [72] S. Scheiner, *Acc. Chem. Res.* **2012**, *46*, 280.
- [73] Q. Li, H. Wang, Z. Liu, W. Li, J. Cheng, B. Gong, J. Sun, *J. Phys. Chem. A* **2009**, *113*, 14156.
- [74] Y. Li, D. Wu, Z.-R. Li, W. Chen, C.-C. Sun, *J. Chem. Phys.* **2006**, *125*, 084317.
- [75] K. Yuan, Y. Zhu, Y. Liu, Z. Li, X. Dong, X. Wang, H. Li, J. Zhang, *Chin. Sci. Bull.* **2008**, *53*, 3151.
- [76] S. Ohta, Y. Ohki, Y. Ikagawa, R. Suizu, K. Tatsumi, *J. Organomet. Chem.* **2007**, *692*, 4792.
- [77] L. Guan, Y. Mo, *J. Phys. Chem. A* **2014**, *118*, 8911.
- [78] H. Georg, E. Fileti, T. Malaspina, *J. Mol. Model.* **2013**, *19*, 329.
- [79] M. Rezaei, K. H. Michaelian, N. Moazzen-Ahmadi, A. R. W. McKellar, *J. Phys. Chem. A* **2013**, *117*, 13752.
- [80] H. Ossor, M. Pfeffer, J. T. B. H. Jastrzebski, C. H. Stam, *Inorg. Chem.* **1987**, *26*, 1169.
- [81] S. J. Grabowski, *Phys. Chem. Chem. Phys.* **2014**, *16*, 1824.
- [82] R. Q. Pordeus, D. G. Rego, B. G. Oliveira, *Spectrochim. Acta A Mol. Biomol. Spectrosc.* **2015**, *145*, 580.
- [83] B. A. Chalmers, M. Bühl, K. S. Athukorala Arachchige, A. M. Z. Slawin, P. Kilian, *Chem. Eur. J.* **2015**, *21*, 7520.
- [84] M. Oestreich, J. Hermeke, J. Mohr, *Chem. Soc. Rev.* **2015**, *44*, 2202.
- [85] D. Roca-López, V. Polo, T. Tejero, P. Merino, *J. Org. Chem.* **2015**, *80*, 4076.
- [86] S. J. Grabowski, *Phys. Chem. Chem. Phys.* **2013**, *16*, 1824.
- [87] R. Liu, P. J. Loll, R. G. Eckenhoff, *FASEB J.* **2005**, *19*, 567.

Received: 14 May 2015

Revised: 5 July 2015

Accepted: 7 July 2015

Published online on 17 August 2015